

Localized-magnetic-moment theory of Fe-Ni Invar

J. M. Wesselinowa and I. P. Ivanov

Department of Physics, University of Sofia, Blvd. J. Bouchier 5, 1126 Sofia, Bulgaria

P. Entel

University of Duisburg, FB 10, Theoretical Lowtemperaturephysics, Lotharstrasse 1, 47048 Duisburg, Germany

(Received 26 July 1996; revised manuscript received 27 September 1996)

A Green's function technique for localized magnetic moments coupled to lattice degrees of freedom is used to study the moment-volume instability in Invar alloys. We present calculations of the total energy as function of volume, magnetic moment, and alloy concentration incorporating both longitudinal and transverse spin fluctuations. For ordered Fe₃Ni, the total energy as function of volume consists of two separate but crossing branches corresponding to the low-spin (LS) and high-spin (HS) states, with a discontinuous magnetic moment at the crossing. With increasing temperature we find that the LS and HS states come closer and finally merge at a critical temperature. In addition, the temperature dependence of the magnetic contribution to the relative volume change ω_m has been calculated in the presence of an external magnetic field. We have extended the calculations to off-stoichiometric concentrations of the alloy system Fe_xNi_{1-x} and present results for the temperature and concentration variation of the thermal expansion coefficient α_m and of the energy difference between the LS and the HS state. Theoretical results compare fairly well with experimental data in spite of using a nonitinerant electron model. [S0163-1829(97)02914-7]

I. INTRODUCTION

During the past years there has been considerable progress in the understanding of moment-volume instabilities in a certain group of fcc $3d$ transition-metal alloys showing a broad spectrum of anomalies often being referred to as Invar anomalies (for recent review articles see Refs. 1 and 2). Most investigated alloys are probably Fe_xNi_{1-x} and Fe_xPt_{1-x} which for certain concentrations x have approximately invariant thermal expansion coefficients over a considerable range of temperatures. Another interesting aspect is that for the Fe-rich alloys, Fe_xNi_{1-x} and other Invar alloys change their crystal structure from fcc to bcc with decreasing temperature (for a detailed discussion of the close relationship of Invar properties and martensitic phase transformations we refer to Ref. 3).

A number of theoretical models have been proposed for describing the Invar effect.⁴⁻⁷ Moruzzi has given a qualitative explanation of the Invar effect and of a number of other properties of Invar alloys which is based on first-principles calculations of model Invar systems like Fe₃Ni, Fe₃Pt, etc., in the fcc structure.^{6,8,9} According to this picture, in pure fcc Fe a low-spin (or paramagnetic-antiferromagnetic) state with a relatively low equilibrium volume is the locally stable state, while at expanded volumes the high-spin state is stable. The resulting binding energy curve as a function of volume consists of two crossing branches corresponding to the low-spin (LS) and the high-spin (HS) state, respectively. As the Ni concentration increases, the difference in energy between LS and HS states decreases, and at a certain concentration the HS state becomes more stable. While this theory (which, in fact, closely resembles the older two-state γ model of Weiss⁴) certainly reproduces basic experimental findings, its treatment of magnetic and lattice degrees of freedom remains on a too qualitative level at finite temperatures. Frozen-

phonon calculations have shown that very small thermal expansion is very likely due to many-body scattering effects with phonon-assisted resonant electronic transitions from strongly antibonding majority-spin t_{2g} states (keeping the atomic volume large due to enhanced partial pressure) into nonbonding minority-spin t_{2g} and e_g states (thereby lowering the atomic volume due to decreasing d -electron partial pressure).^{3,7,10,11} This opens a pseudogap in the minority spin density of states hindering further substantial thermal expansion since electrons have to overcome this energy barrier. Note that a similar pseudogap exists in the (s,p) -bonded nonmagnetic Hume-Rothery alloys due to many-electron scattering on the Bragg planes of the new crystal structure close to the bcc-fcc phase transition.

This brief discussion shows that finite-temperature first-principles calculations of Invar and Hume-Rothery alloys will be needed to further pursue in detail the physics of Invar and structural transformations in magnetic and nonmagnetic alloys. In addition, finite temperatures will involve the big impact of multiphonon processes and of the electron-phonon interaction on itinerant magnetism in general¹² and on the thermal expansion in particular.³ Besides from tentative not parameter-free molecular-dynamics calculations,¹³ these kinds of calculations would require enormous computational efforts. Therefore, the extension of *ab initio* results to finite temperatures has been achieved by less tedious calculations using a Gaussian theory of spin and volume fluctuations at finite temperatures (as an extension of the mode-mode coupling theory of Murata and Doniach¹⁴) based on a Ginzburg-Landau theory with zero-temperature *ab initio* data as input.^{3,7,15-19} This phenomenological theory allows one to extend the zero-temperature binding surfaces to finite temperatures and to explore the mutual influence of longitudinal and transverse spin fluctuations and of charge (volume) fluctuations. It is found that transverse spin fluctuations contrib-

ute in an essential way to the Invar anomaly in Fe-Ni and Fe-Pt in accordance with earlier work by Moriya and Usami who used a more simplified scheme to discuss the expansion anomaly.²⁰ In this context it should be mentioned that also results of first-principles coherent-potential approximation (CPA) calculations for the case of off-stoichiometric alloys^{3,21,22} can be extended to finite temperatures allowing for a rough evaluation of temperature- and concentration-dependent phase diagrams. In addition, the CPA calculations allow for a detailed investigation of the competition between the LS and the HS state as function of alloy concentration. The theoretical results nearly agree quantitatively with experiment.³ Also, this kind of continuing *ab initio* zero-temperature results to finite temperatures allows one to treat Invar and anti-Invar behavior on equal footing.

In this paper we extend the forgoing finite-temperature calculations by making use of a localized magnetic moment model in which the magnetic moments are coupled in the same phenomenological way as previously to the lattice. We compensate for the neglect of the picture of itinerant magnetism by a rather subtle decoupling of the spin Green's function by using the technique of Tserkovnikov.²³ This procedure allows one in a nice way to deal with alloys yielding concentration dependent nonintegral values for the magnetization. For $\text{Fe}_{1-x}\text{Ni}_x$ we present calculations of the total energy as function of the volume, the magnetic moment, and the Ni concentration by incorporating both longitudinal and transverse spin fluctuations. The final aim of using a localized magnetic moment model is to incorporate phonons in a phenomenological way by allowing for Lennard-Jones type of interactions between the Fe and Ni atoms. The model can then be solved exactly by a Monte Carlo step simulation technique for spin and phonons.²⁴⁻²⁵ In particular, this model allows for an investigation of the critical behavior (calculation of critical indices and scaling relations for the coupled spin-phonon system). This is beyond the scope of this paper and will be published elsewhere.²⁵

II. THE MODEL

The Hamiltonian of the system Fe_3Ni can be written as (a similar model was used by Dube *et al.*²⁶)

$$H = H_M + H_{\text{MV}} + H_V. \quad (1)$$

H_M is the Heisenberg Hamiltonian for $\text{Fe}=f$ and $\text{Ni}=n$ and the interaction between them;

$$H_M = -g\mu_B H \sqrt{N}(S_0^{fz} + S_0^{nz}) - \frac{1}{2} \sum_{\mathbf{q}} J_{\mathbf{q}}^{ff} \mathbf{S}_{-\mathbf{q}}^f \cdot \mathbf{S}_{\mathbf{q}}^f - \frac{1}{2} \sum_{\mathbf{q}} J_{\mathbf{q}}^{nn} \mathbf{S}_{-\mathbf{q}}^n \cdot \mathbf{S}_{\mathbf{q}}^n - \frac{1}{2} \sum_{\mathbf{q}} J_{\mathbf{q}}^{fn} \mathbf{S}_{-\mathbf{q}}^f \cdot \mathbf{S}_{\mathbf{q}}^n. \quad (2)$$

The magnetovolume coupling is given by the second term H_{MV} ,

$$H_{\text{MV}} = -\frac{1}{2} \sum_{\mathbf{q}} [D_0(\mathbf{q})\omega + D_1(\mathbf{q})\omega^2] \mathbf{S}_{-\mathbf{q}}^f \cdot \mathbf{S}_{\mathbf{q}}^n, \quad (3)$$

where ω is the relative volume $[V(T) - V_0]/V_0$ with V_0 being the volume of the hypothetical nonmagnetic ground state.

Here we take for brevity only the quadratic terms in the spin density. Although this is reasonable for weak magnets, we can easily take account of higher-order terms if necessary.

Finally, H_V is the harmonic lattice term

$$H_V = \frac{B}{2} \omega^2. \quad (4)$$

The magnetic contribution to the thermal expansion is given by

$$\omega_m = \sum_{\mathbf{q}} \frac{D_{\mathbf{q}}}{B} (\langle S_{\mathbf{q}}^2 \rangle_T - \langle S_{\mathbf{q}}^2 \rangle_0), \quad (5)$$

where B is the bulk modulus and $\langle \dots \rangle_T$ means the statistical average at temperature T . In weakly ferromagnetic metals, where small \mathbf{q} components of spin fluctuations are predominant, we may approximate $D_{\mathbf{q}} \sim D_0$ and get²⁷

$$\omega_m(T) = N_0^2 \frac{D_0}{B} [S_L^2(T) - S_L^2(0)], \quad (6)$$

where N_0 is the number of atoms in the crystal; S_L^2 is the mean-square local amplitude of spin fluctuations. A fair interpolation between $T=0$ and T_c may be

$$\omega_m(T) = \frac{2}{5} \frac{D_0}{B} [M^2(T) - M^2(0)], \quad (7)$$

for $T < T_c$, M is the spontaneous magnetization. The relative volume change due to an external magnetic field is then given by

$$\omega(H, T) = \frac{2}{5} \frac{D_0}{B} [M^2(H, T) - M^2(0, T)]. \quad (8)$$

III. CALCULATION OF THE TOTAL ENERGY

In the following we will calculate the total energy with the help of the retarded Green's function defined in matrix form as

$$\tilde{G}_{\mathbf{k}}(t) = i\Theta(t) \langle [B_{\mathbf{k}}(t), B_{\mathbf{k}}^{\dagger}] \rangle. \quad (9)$$

The operator $B_{\mathbf{k}}$ stands symbolically for the set $S_{\mathbf{k}}^{f+}$, $S_{\mathbf{k}}^{n+}$, $S_{\mathbf{k}}^{fz}$. For the approximate calculation of the Green's function (9) we use a method proposed by Tserkovnikov.²³ The energy in the generalized Hartree-Fock approximation is given by

$$E(\mathbf{k}) = \langle [[B_{\mathbf{k}}, H], B_{\mathbf{k}}^{\dagger}] \rangle / \langle [B_{\mathbf{k}}, B_{\mathbf{k}}^{\dagger}] \rangle \quad (10)$$

Using Eq. (10) we obtain for the transverse and longitudinal spin-wave energy of Fe_3Ni , respectively (taking into account both longitudinal and transverse spin fluctuations):

$$E(\mathbf{k}) = \frac{1}{2} [\epsilon_{11} + \epsilon_{22} \pm \sqrt{(\epsilon_{11} - \epsilon_{22})^2 + 4\epsilon_{12}\epsilon_{21}}], \quad (11)$$

$$E_l(\mathbf{k}) = \epsilon_{33}, \quad (12)$$

with the matrix elements

$$\begin{aligned} \epsilon_{11}(\mathbf{k}) = & g\mu_B H + \frac{1}{2\langle S^{fz} \rangle} \left(\frac{1}{N} \sum_{\mathbf{q}} J_{\mathbf{q}}^{fn} (\langle S_q^{f-} S_q^{n+} \rangle + 2\langle S_q^{fz} S_q^{nz} \rangle) + \frac{1}{N} \sum_{\mathbf{q}} (D_q^0 \omega + D_q^1 \omega^2) (\langle S_q^{f-} S_q^{n+} \rangle + 2\langle S_q^{fz} S_q^{nz} \rangle) \right. \\ & \left. + \frac{1}{N} \sum_{\mathbf{q}} (J_q^{ff} - J_{k-q}^{ff}) (2\langle S_q^{fz} S_{-q}^{fz} \rangle + \langle S_{k-q}^{f-} S_{k-q}^{f+} \rangle) \right), \end{aligned} \quad (13)$$

$$\epsilon_{12}(\mathbf{k}) = -\frac{1}{2\langle S^{nz} \rangle} \left(\frac{1}{N} \sum_{\mathbf{q}} J_{\mathbf{q}}^{fn} (\langle S_{k-q}^{n-} S_{k-q}^{f+} \rangle + 2\langle S_{k-q}^{fz} S_{q-k}^{nz} \rangle) + \frac{1}{N} \sum_{\mathbf{q}} (D_q^0 \omega + D_q^1 \omega^2) (\langle S_{k-q}^{n-} S_{k-q}^{f+} \rangle + 2\langle S_{k-q}^{fz} S_{q-k}^{nz} \rangle) \right), \quad (14)$$

$$\epsilon_{21}(\mathbf{k}) = -\frac{1}{2\langle S^{fz} \rangle} \left(\frac{1}{N} \sum_{\mathbf{q}} J_{\mathbf{q}}^{fn} (\langle S_{k-q}^{f-} S_{k-q}^{n+} \rangle + 2\langle S_{k-q}^{fz} S_{q-k}^{nz} \rangle) + \frac{1}{N} \sum_{\mathbf{q}} (D_q^0 \omega + D_q^1 \omega^2) (\langle S_{k-q}^{f-} S_{k-q}^{n+} \rangle + 2\langle S_{k-q}^{fz} S_{q-k}^{nz} \rangle) \right), \quad (15)$$

$$\begin{aligned} \epsilon_{22}(\mathbf{k}) = & g\mu_B H + \frac{1}{2\langle S^{nz} \rangle} \left(\frac{1}{N} \sum_{\mathbf{q}} J_{\mathbf{q}}^{fn} (\langle S_q^{n-} S_q^{f+} \rangle + 2\langle S_q^{fz} S_q^{nz} \rangle) + \frac{1}{N} \sum_{\mathbf{q}} (D_q^0 \omega + D_q^1 \omega^2) (\langle S_q^{n-} S_q^{f+} \rangle + 2\langle S_q^{fz} S_q^{nz} \rangle) \right. \\ & \left. + \frac{1}{N} \sum_{\mathbf{q}} (J_q^{nn} - J_{k-q}^{nn}) (2\langle S_q^{nz} S_{-q}^{nz} \rangle + \langle S_{k-q}^{n-} S_{k-q}^{n+} \rangle) \right), \end{aligned} \quad (16)$$

$$\epsilon_{33}(\mathbf{k}) = \frac{1}{2\langle S_{\mathbf{k}}^{fz} S_{-\mathbf{k}}^{fz} \rangle N} \sum_{\mathbf{q}} [(J_q^{ff} - J_{k-q}^{ff}) \langle S_q^{f-} S_q^{f+} \rangle + (J_q^{fn} + D_q^0 \omega + D_q^1 \omega^2) \langle S_q^{f-} S_q^{n+} \rangle]. \quad (17)$$

The correlation functions are calculated to

$$\begin{aligned} n_{\mathbf{q}}^f = \langle S_{\mathbf{q}}^{f-} S_{\mathbf{q}}^{f+} \rangle = & \frac{\langle S^{fz} \rangle}{2\omega_{\mathbf{q}}^2} [(\omega_{\mathbf{q}}^2 - \epsilon_{\mathbf{q}}^{13} \epsilon_{\mathbf{q}}^{31}) (\Phi_1 + \Phi_2) \\ & + \omega_{\mathbf{q}} \epsilon_{\mathbf{q}}^{11} (\Phi_1 - \Phi_2)], \end{aligned} \quad (18)$$

$$\langle S_{\mathbf{q}}^{fz} S_{-\mathbf{q}}^{fz} \rangle = \frac{1 + 2\bar{n}_{\mathbf{q}}^f + 2\bar{n}_{\mathbf{q}}^{f2}}{1 + 3\bar{n}_{\mathbf{q}}^f + 3\bar{n}_{\mathbf{q}}^{f2}}. \quad (19)$$

Further we have used the abbreviations $\omega_{\mathbf{q}} = \sqrt{E_{\mathbf{q}}^2 + 2\epsilon_{\mathbf{q}}^{13} \epsilon_{\mathbf{q}}^{31}}$, $\Phi_1 = \exp(\omega_{\mathbf{q}}/T)^{-1}$, $\Phi_2 = [\exp(-\omega_{\mathbf{q}}/T) - 1]^{-1}$. We obtain for ϵ_k^{13} and ϵ_k^{31} the following expressions, respectively:

$$\begin{aligned} \epsilon_{\mathbf{k}}^{13} = & \frac{1}{2\langle S^{fz} \rangle N} \sum_{\mathbf{q}} [(J_q^{ff} - J_{q-k}^{ff}) \langle S_{q-k}^{f-} S_{q-k}^{fz} \rangle \\ & - (J_q^{fn} + D_q^0 \omega + D_q^1 \omega^2) \langle S_q^{n+} S_{-q}^{fz} \rangle], \end{aligned} \quad (20)$$

$$\begin{aligned} \epsilon_{\mathbf{k}}^{31} = & \frac{1}{2\langle S_{\mathbf{k}}^{fz} S_{-\mathbf{k}}^{fz} \rangle N} \sum_{\mathbf{q}} [(J_q^{ff} - J_{k-q}^{ff}) \langle S_{k-q}^{f+} S_{q-k}^{fz} \rangle \\ & - (J_q^{fn} + D_q^0 \omega + D_q^1 \omega^2) \langle S_q^{f+} S_{-q}^{nz} \rangle] \end{aligned} \quad (21)$$

with the correlation function

$$\begin{aligned} \langle S_{\mathbf{q}}^{f+} S_{-\mathbf{q}}^{fz} \rangle = \langle S_{\mathbf{q}}^{fz} S_{\mathbf{q}}^{f-} \rangle = & \frac{\langle S^{fz} \rangle^2 \epsilon_{\mathbf{q}}^{31} \epsilon_{\mathbf{q}}^{13}}{\omega_{\mathbf{q}}^2} [\omega_{\mathbf{q}} (\Phi_1 - \Phi_2) \\ & + (\epsilon_{\mathbf{q}}^{11} - \epsilon_{\mathbf{q}}^{12}) (\Phi_1 + \Phi_2)]. \end{aligned} \quad (22)$$

In the RPA we obtain for the matrix elements ϵ_{ij}

$$\begin{aligned} \epsilon_{11}(\mathbf{k}) = & g\mu_B H + \langle S^{nz} \rangle (J_0^{fn} + D_0 \omega + D_1 \omega^2) \\ & + \langle S^{fz} \rangle (J_0^{ff} - J_{\mathbf{k}}^{ff}), \end{aligned} \quad (23)$$

$$\epsilon_{12}(\mathbf{k}) = -\langle S^{fz} \rangle (J_{\mathbf{k}}^{fn} + D_0 \omega + D_1 \omega^2), \quad (24)$$

$$\epsilon_{21}(\mathbf{k}) = -\langle S^{nz} \rangle (J_{\mathbf{k}}^{fn} + D_0 \omega + D_1 \omega^2), \quad (25)$$

$$\begin{aligned} \epsilon_{22}(\mathbf{k}) = & g\mu_B H + \langle S^{fz} \rangle (J_0^{fn} + D_0 \omega + D_1 \omega^2) \\ & + \langle S^{nz} \rangle (J_0^{nn} - J_{\mathbf{k}}^{nn}), \end{aligned} \quad (26)$$

$$\epsilon_{33}(\mathbf{k}) = 0. \quad (27)$$

There is a solution with $\epsilon_{33}=0$. It corresponds to the longitudinal mode, i.e., a relaxation of the spin components parallel to the mean field.

$\langle S^{fz} \rangle$ and $\langle S^{nz} \rangle$ are the relative magnetization of Fe and Ni, respectively:

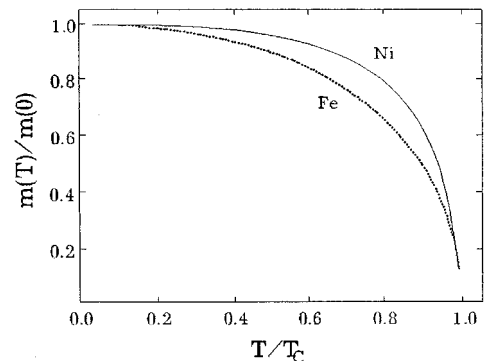


FIG. 1. Temperature dependence of the relative magnetization of Ni (solid line) and Fe (dashed line) in Fe_3Ni .

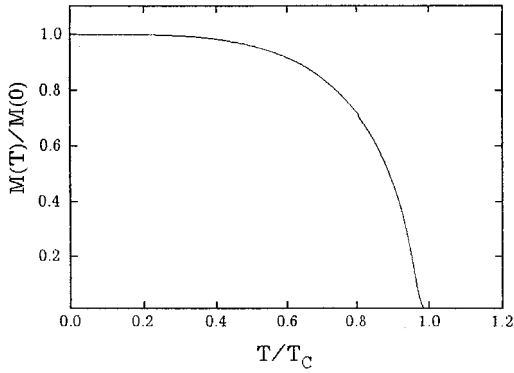


FIG. 2. Temperature dependence of the magnetization/atom of Fe_3Ni .

$$m^{f,n} = \langle S^{f,nz} \rangle = \frac{1}{N} \sum_k \left\{ \left(S^{f,n} + \frac{1}{2} \right) \coth \left[\left(S^{f,n} + \frac{1}{2} \right) \beta E_k \right] - \frac{1}{2} \coth \left(\frac{1}{2} \beta E_k \right) \right\}, \quad (28)$$

where $S^f=2$ and $S^n=0.5$. For the magnetization/atom we obtain

$$M(T) = \frac{1}{4} (3m^f + m^n). \quad (29)$$

IV. NUMERICAL RESULTS AND DISCUSSION

First we have calculated the temperature dependence of the relative magnetization of Fe and Ni in Fe_3Ni and of the magnetization/atom of Fe_3Ni with following parameters: $J^{fn}=0.0316$ eV, $J^{ff}=-0.00995$ eV, $J^{nn}=0.0158$ eV, $D_0=0.017$ eV, $D_1=0.3$ eV which were obtained by fitting the curves of Moruzzi.⁶ The results are shown in Figs. 1 and 2, respectively.

We will compare the longitudinal spin fluctuations (LSF's) and the spin-wave contribution to the magnetization $M(T)$. $M(T)$ is plotted in Fig. 3, where curve 1 is calculated taking into account spin waves and LSF, whereas curve 2 is calculated with spin waves only. One can see that LSF and spin waves equally influence the temperature dependence of the magnetization $M(T)$. If we neglect the LSF, then we

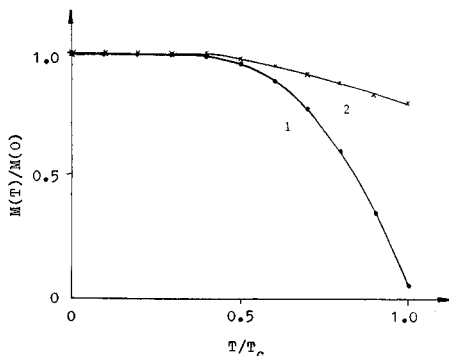


FIG. 3. Temperature dependence of the magnetization $M(T)/M(0)$ taking into account (1) LSF and transverse spin waves (2) only spin waves.

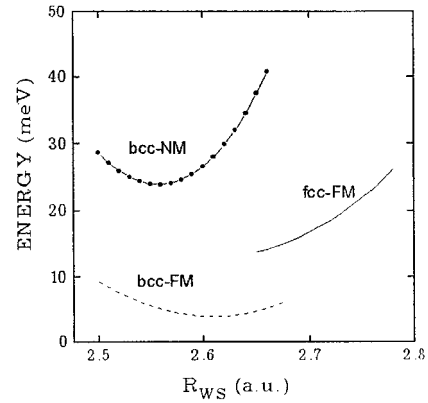


FIG. 4. Zero-magnetic field total energy vs Wigner-Seitz radius R_{WS} for bcc and fcc Fe ($T=0$) in different magnetic structures: NM, nonmagnetic; FM, ferromagnetic. In the fcc form, the NM phase is stable for $R_{\text{WS}} \leq 2.65$ a.u. and the HS phase is stable for $R_{\text{WS}} \geq 2.67$ a.u.

obtain curve 2, which decreases much more slowly than experimentally obtained.^{28,29} The spin waves are therefore not enough to account for the anomalous temperature variation of the magnetization. The conventional explanation for the observed behavior is that there are additional ‘‘hidden’’ excitations which participate in reducing the magnetization. One possibility is that the (transverse) spin-wave excitations couple to the longitudinal spin-wave energies. $M(T)/M(0)$ increases against T/T_c with increasing Ni concentration for Fe-Ni alloys, in agreement with the experimental data.³⁰ In $\text{Fe}_{50}\text{Ni}_{50}$, which has no Invar effect, we obtain good agreement with the experimental data taking into account only the influence of the spin waves. The contribution of these ‘‘hidden’’ excitations on the spin dynamics of Fe-Ni Invar alloys which may help to explain the Invar anomaly will be discussed elsewhere.³¹

A way of displaying pertinent phase information is to show total energies versus volume (or R_{WS}), or lines corresponding to minimum energies for fixed volumes. Although the case of fcc Fe has received theoretical attention before, we want to begin with this case. This will set the stage for

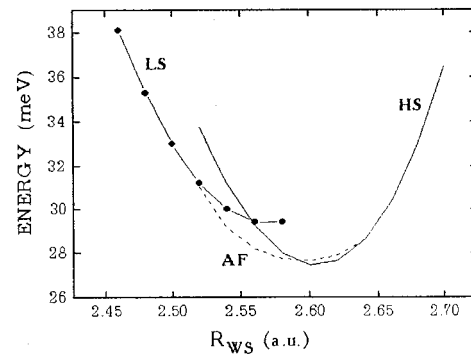


FIG. 5. Zero-magnetic field total-energy fixed-spin-moment results for Fe_3Ni vs R_{WS} ($T=0$). The instability is induced by the crossing of the LS and HS total-energy branches. The dashed curve is an assumed antiferromagnetic branch, which is required to explain the initial negative low-temperature expansion in Invar.

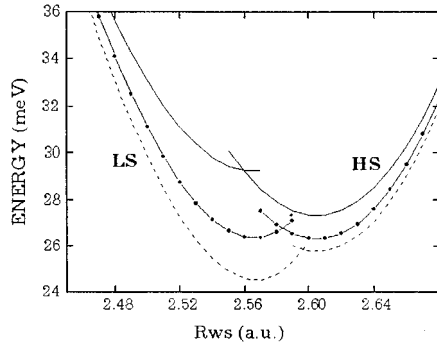


FIG. 6. Thermal evolution of the two branches of the LS and HS states for Invar: solid line, $T=100$ K points, 177 K dashed line, 200 K. The LS and HS states merge at $T \approx 177$ K.

our results concerning Fe_3Ni which we will contrast with those of fcc Fe. Figure 4 shows the zero-field total energy $E_{\mathbf{k}}^f$ with $J_{\mathbf{q}}^{fn} = J_{\mathbf{q}}^{nn} = 0$ of bcc and fcc Fe in different magnetic structures (NM represents nonmagnetic and FM represents ferromagnetic) as a function of the Wigner-Seitz radius R_{WS} , which is used as a measure of the volume $V = (4\pi/3)R_{\text{WS}}^3$. The results are in agreement with those of Moruzzi.^{8,32} It should be noted that Uhl *et al.*¹⁹ obtain for fcc Fe a lower value of E as compared to bcc Fe. This is known to be a LDA defect that disappears in Moruzzi³² and in our work. It can be seen from Fig. 4 that the magnetic structure depends sensitively on the volume. Our calculations give locally stable configurations at $2.61 < R_{\text{WS}} < 2.65$ a.u. and at $2.67 < R_{\text{WS}} < 2.72$ a.u., which are in agreement with neutron-diffraction experiments on γ -Fe precipitates in copper.^{33,34} In the fcc structure, the NM phase is stable for $R_{\text{WS}} \leq 2.65$ a.u. and the HS phase is stable for $R_{\text{WS}} \geq 2.67$ a.u.

We will now consider stoichiometrically ordered Fe_3Ni as a ‘‘model’’ Invar system even though we know that true Invar is chemically disordered and has a slightly different stoichiometry. The calculation yields the zero-field results of $E_{\mathbf{k}}$ shown in Fig. 5 with increasing volume (or R_{WS}). We find that the total energy must be represented as two separate but crossing branches with a discontinuous magnetic moment at the crossing. The magnetic instability is indicated by the crossing of the LS and HS total-energy branches because the system can be in either magnetic state with no change in

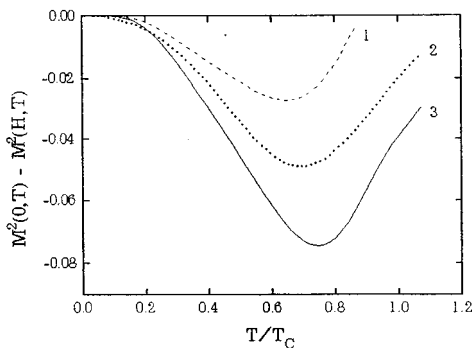


FIG. 7. The temperature dependence of the relative volume change due to different magnetic field values dashed line, $R=0.945$ at. %; points, 0.63 mT; solid line, 1.26 mT.

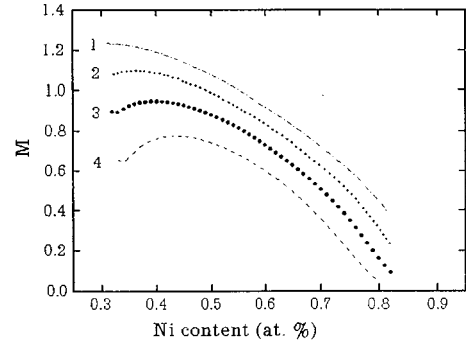


FIG. 8. Dependence of the magnetization/atom on the Ni concentration for different temperature values: (1) $T=300$ K, (2) 350 K, (3) 400 K, (4) 450 K.

energy. The dashed curve is an assumed antiferromagnetic branch, as reported in the works of Moruzzi,⁶ which is required to explain the initial negative low-temperature thermal expansion in Invar. The existence of such a spin state is experimentally still not established. Therefore, it would be not considered by the investigation of the state behavior of different temperatures. The two branches are physically similar to the Weiss 2γ -state Invar model.⁴ The resulting instability occurs at a volume below the absolute energy minimum which corresponds to the HS state. Because this is a two-component system, the situation is more complicated than in elemental fcc Fe (Fig. 4). For small volumes the system is in a nonmagnetic state. At a Wigner-Seitz radius of $R_{\text{WS}}=2.46$ a.u., the LS state starts and is found as a single minimum in the total energy versus R_{WS} . The HS state appears at $R_{\text{WS}}=2.52$ a.u. In the volume range $R_{\text{WS}}=2.52-2.58$ a.u., we found coexistence of both the LS and HS states. The $E(V)$ curve describing this two-phase region has two minima at the respective R_{WS} . For $R_{\text{WS}} > 2.58$ a.u., the LS state disappears and only the HS solution remains. The equilibrium volume is found at about $R_{\text{WS}}=2.6$ a.u., where only the HS state exists. Note that the difference in energy between the HS and the LS state is about 1.1 mRy, implying a characteristic Invar temperature of about 170 K. Thus, with increasing temperature a plausible explanation for the Invar behavior results. Figure 5 shows zero-magnetic-field results for the

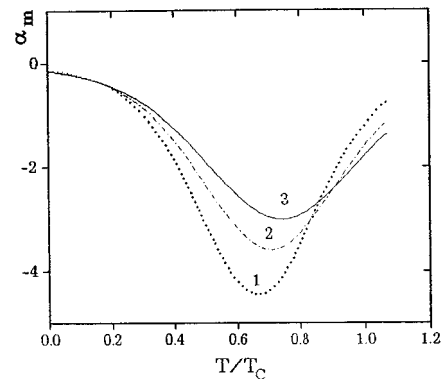


FIG. 9. The thermal expansion coefficient α_m as a function of the temperature for different Ni concentration values, x : (1) $x=0.35$ at. %, (2) $x=0.40$ at. %, (3) $x=0.45$ at. %.

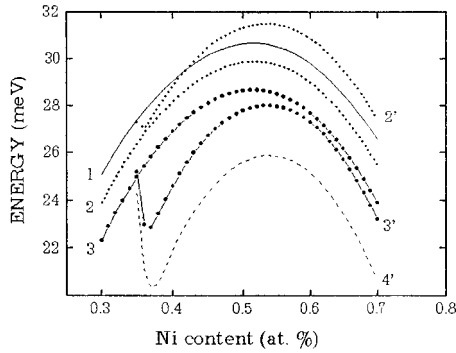


FIG. 10. The energy for the LS state, with prime, and for the HS state, without prime, as a function of the Ni concentration for different T values: (1) $T=100$ K, (2) 177 K, (3) 200 K, (4) 230 K.

total energy being in good agreement with other works.^{6,7,36} The FM ground state of Fe_3Ni has a larger volume than the NM state which lies slightly higher in energy.

With increasing temperature we find that the LS and the HS states come closer and finally merge at T_c (Fig. 6). At low temperatures the HS high-volume branch determines the ground state. At higher temperatures the LS low-volume branch determines the ground state. A similar behavior for the free energy was found by Moruzzi.⁹ The minimum of the HS state remains nearly at the same R_{WS} , whereas the minimum of the LS state shifts to higher R_{WS} values. It is clear that the LS state is attended not only with variation of the energy minimum, but with change of the equilibrium primitive cell volume, too, where the energy as a function of the relative volume at $T=\text{const}$ has a minimum. At temperatures about $0.7T_c$ this volume occurs commensurable with the equilibrium value of the HS state at $T=0$. On the other hand, at this temperature T there exists a maximum in the magnetic contribution to the thermal expansion coefficient α_m (see Fig. 9). That is why we make a guess that the variation of the equilibrium parameter of the crystal lattice for LS in relation to this for HS is the reason for presence of peculiarity in the thermal behavior of the Invar alloy.

In Fig. 7 is shown the temperature dependence of the relative volume change due to different magnetic field values. With increasing h the minimum shifts to higher T values and smaller ω_m values. The reason of such behavior is the influence of the field on T_c , on the one hand, and on the magnetic moment value, on the other hand.

Finally we have made some calculations for the alloy $\text{Fe}_x\text{Ni}_{1-x}$, too. Evidence for the magnetic origin of Invar behavior is provided by Fig. 8 which shows the concentration dependence of the magnetization/atom M in Fe-Ni alloys. In agreement with Yamada and Nakai,³⁵ and Williams *et al.*³⁶ Invar behaviour is confined to concentrations near $\approx 35\%$, where we see a dramatic deviation of the magnetization from the Slater-Pauling curve. The maximum shifts to smaller Ni concentrations with decreasing temperature T . With increasing T the magnetic moment decreases. Figure 9 shows the temperature dependence of the thermal expansion coefficient α_m , which is the derivative of ω_m , for different Ni-concentration values. These are in very good agreement with the experimental data. The largest changes are at temperatures about $0.7T_c$, which corroborates that mentioned

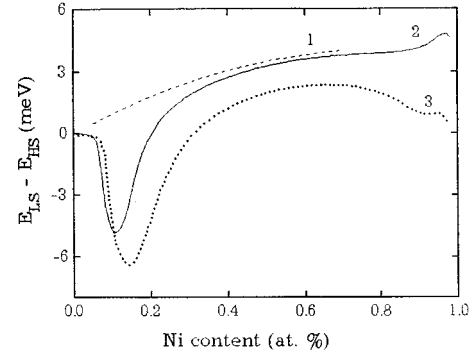


FIG. 11. Energy difference between the LS and the HS states, $E_{\text{LS}} - E_{\text{HS}}$, of the Fe-Ni alloy as a function of the Ni concentration for different temperatures: (1) $T=0$ K, (2) 130 K, (3) 170 K.

above, that the magnetic volume effects of the considered Invar alloy are important at $T \approx 0.7T_c$ (see Fig. 6). Obviously, the influence of α_m at temperatures near and specially above T_c is small. Therefore the Invar alloys show this anomaly only for $T < T_c$. At higher Ni concentration, the magnetic contribution to the thermal expansion decreases. The concentration dependence of the energy of the two spin states LS and HS is plotted in Fig. 10. The curves show a maximum, whereas the LS states have, besides this, a minimum in a small Ni concentration interval from ≈ 0.35 to 0.4 at. % Ni for temperatures above $T_{\text{HS} \rightarrow \text{LS}}$. This peculiarity determines the magnetic ordered state of the system. In Fig. 11 is plotted the energy difference between LS and HS state as a function of the alloy concentration for different temperature values. At temperatures about $T \approx 0$ K for all concentration values, HS is the only stable state. For higher temperatures a competition appears between LS and HS, and the temperature of the transition $\text{HS} \rightarrow \text{LS}$ is different for different concentration values. For Ni concentration, $x_1 \approx 0.35$ at. % of the alloy the temperature at which E_{HS} is equal to E_{LS} is about $T \approx 170$ K.

V. CONCLUSIONS

Using a Green's function technique for localized magnetic moments coupled to the lattice degrees of freedom, we have studied the moment-volume instability in Invar alloys. The total energy is calculated as a function of volume, magnetic moment, and alloy concentration incorporating both longitudinal and transverse spin fluctuations. For ordered Fe_3Ni the total energy as a function of volume consists of two separate but crossing branches corresponding to the LS and HS states, with a discontinuous magnetic moment at the crossing. With increasing temperature we find that the LS and the HS states come closer and finally merge at a critical temperature. In addition, the temperature dependence of the relative volume change ω_m in the presence of an external magnetic field has been obtained. Furthermore we have taken into account off-stoichiometric concentration of the alloy system $\text{Fe}_x\text{Ni}_{1-x}$. With increase of the Ni concentration x , ω_m increases too. The thermal expansion coefficient α_m and the energy difference between the LS and the HS state as a function of T and x are discussed. The theoretical results are in good agreement with experimental data.

- ¹E. F. Wassermann, in *Ferromagnetic Materials*, edited by K. H. J. Buschow and E. P. Wohlfarth (North-Holland, Amsterdam, 1990), Vol. 5, p. 237.
- ²M. Shiga, in *Materials Science and Technology*, edited by R. W. Cahn, P. Haasen, and E. J. Kramer (VCH, Weinheim, 1994), Vol. 3B, p. 159.
- ³M. Schröter, H. Ebert, H. Akai, P. Entel, E. Hoffmann, and G. G. Reddy, *Phys. Rev. B* **52**, 188 (1995).
- ⁴R. J. Weiss, *Proc. R. Soc. London* **82**, 281 (1963).
- ⁵J. Kaspar and D. R. Salahuh, *Phys. Rev. Lett.* **47**, 54 (1981).
- ⁶V. L. Moruzzi, *Physica B* **161**, 99 (1989).
- ⁷P. Entel, E. Hoffmann, P. Mohn, K. Schwarz, and V. L. Moruzzi, *Phys. Rev. B* **47**, 8706 (1993).
- ⁸V. L. Moruzzi, *Phys. Rev. B* **41**, 6939 (1990).
- ⁹V. L. Moruzzi, *Solid State Commun.* **83**, 739 (1992).
- ¹⁰E. Hoffmann, P. Entel, K. Schwarz, and P. Mohn, *J. Magn. Magn. Mater.* **140-144**, 237 (1995).
- ¹¹H. C. Herper, P. Entel, and W. Weber, *J. Phys. Pans (Colloq.)* **56**, C2-129 (1995).
- ¹²D. J. Kim, *Phys. Rep.* **171**, 129 (1988).
- ¹³R. Meyer and P. Entel, *J. Phys. Pans (Colloq.)* **56**, C2-123 (1995).
- ¹⁴K. K. Murala and S. Doniach, *Phys. Rev. Lett.* **29**, 285 (1972).
- ¹⁵P. Entel and M. Schröter, *Physica B* **161**, 160 (1989).
- ¹⁶D. Wagner, *J. Phys. Condens. Matter* **1**, 4635 (1989).
- ¹⁷M. Schröter, P. Entel, and S. G. Mishra, *J. Magn. Magn. Mater.* **87**, 163 (1990).
- ¹⁸P. Mohn, K. Schwarz, and D. Wagner, *Phys. Rev. B* **43**, 3318 (1991).
- ¹⁹M. Uhl, L. M. Sandratskii, and J. Kübler, *Phys. Rev. B* **50**, 291 (1994).
- ²⁰T. Moriya and K. Usami, *Solid State Commun.* **34**, 95 (1980).
- ²¹H. Akai and P. H. Dederichs, *Phys. Rev. B* **47**, 8739 (1993).
- ²²I. A. Abrikosov, O. Eriksson, P. Söderlind, H. L. Skriver, and B. Johansson, *Phys. Rev. B* **51**, 1058 (1995).
- ²³Yu. A. Tserkovnikov, *Teor. Math. Fiz.* **7**, 250 (1971).
- ²⁴M. Gruner, Diploma work, Duisburg, 1995.
- ²⁵M. Gruner, R. Meyer, and P. Entel (unpublished).
- ²⁶M. Dube, P. R. L. Heron, and D. G. Rancourt, *J. Magn. Magn. Mater.* **147**, 122 (1995); **147**, 133 (1995).
- ²⁷T. Moriya, *Spin Fluctuations in Itinerant Electron Magnetism* (Springer, Berlin, 1985).
- ²⁸I. Nakay and O. Yamada, *J. Magn. Magn. Mater.* **31-34**, 103 (1983).
- ²⁹A. K. Zatopylaev, A. Z. Menshikov, and S. V. Podgornykh, *Physics B* **161**, 103 (1983).
- ³⁰J. Crangle and G. C. Hallam, *Proc. R. Soc. A* **272**, 119 (1963).
- ³¹J. M. Wesselinowa, *Phys. Rev. B* **55**, 5608 (1997).
- ³²V. L. Moruzzi, P. M. Marcus, K. Schwarz, and P. Mohn, *Phys. Rev. B* **34**, 1784 (1986).
- ³³Y. Tsunoda, *J. Phys. Condens. Matter* **1**, 10427 (1989).
- ³⁴Y. Tsunoda, *Prog. Theor. Phys. Suppl.* **101**, 133 (1990).
- ³⁵O. Yamada and I. Nakai, *J. Phys. Soc. Jpn.* **50**, 823 (1981).
- ³⁶A. R. Williams, V. L. Moruzzi, C. D. Gelatt Jr., and J. Kübler, *J. Magn. Magn. Mater.* **31-34**, 88 (1983).